A multi-technique approach using LC–NMR, LC–MS, semi-preparative HPLC, HR–NMR and HR–MS for the isolation and characterization of low-level unknown impurities in GW876008, a novel corticotropin-release factor 1 antagonist

Stefano Provera [a,*], Luca Rovatti [a], Lucilla Turco [a], Sebastiano Mozzo [b], Alberto Spezzaferri [b], Sergio Bacchi [b], Arianna Ribecai [b], Simone Guelfi [b], Anna Mingardi [c], Carla Marchioro [a], Damiano Papini [b]

[a] Analytical Chemistry, GlaxoSmithKline Medicines Research Centre, Via Fleming 4, 37135 Verona, Italy
[b] Chemical Development, GlaxoSmithKline Medicines Research Centre, Via Fleming 4, 37135 Verona, Italy
[c] Neuroscience CEDD Synthetic Chemistry, GlaxoSmithKline Medicines Research Centre, Via Fleming 4, 37135 Verona, Italy

ARTICLE INFO

ABSTRACT

A multi-technique approach was applied in order to fully characterize four low-level unknown impurities of GW876008, a novel CRF$_1$ receptor antagonist. Liquid chromatography (LC)–NMR spectroscopy was used in combination with LC–MS to obtain detailed information regarding the structure of the two major impurities present in batches of GW876008 and observed in the first synthetic scale-up for preclinical use. Two additional impurities were unexpectedly found at greater levels in a large scale synthesis for clinical use and their structure was elucidated by means of high resolution (HR)–MS and HR–NMR, after a small scale preparative HPLC purification step. This structural information was useful in terms of shedding light on the typical impurity profile of this new chemical entity with the aim to support the early development package for Phase I clinical studies.

© 2010 Elsevier B.V. All rights reserved.

1. Introduction

CRF$_1$ receptor antagonists are a class of active compounds which were discovered in recent years. These compounds demonstrated biological activity in animal models of behaviour indicating anxiety and depression, by acting on the corticotropin-releasing factor (CRF^a), a 41 amino acid peptide that plays a central role in mediating the behavioural, neuroendocrine, and autonomic responses to stress [1–3]. As part of a thorough exploration aimed at identifying of an innovative series of CRF$_1$ receptor antagonists for the treatment of anxiety and depression, GW876008 (1) was recently reported as a potential lead compound in a wider series of dihydropyrrole[2,3]pyridine analogues [4].

In the development of new medicines, understanding the impurity profile of the Active Pharmaceutical Ingredient (API) is a crucial step in the correct interpretation of the data used to support toxicological and clinical studies, in order to assure quality of drug substance and ultimately patient safety. Knowledge of the structure of the impurities can also provide important insights into the drug development manufacturing process by identifying the chemical reactions responsible for their formation as well as potential degradation pathways [5,6]. This type of information is essential in establishing critical control points in the drug substance synthetic process, thus ensuring its overall quality by setting appropriate in process controls and final API specification limits [7–10].

Regulatory requirements with regard to the identification and control of impurities in the pharmaceutical industry are subject to the International Conference on Harmonization (ICH) Guideline Q3A2, Impurities in New Drug Substances [11] which defines reporting, identification and qualification thresholds for synthetic impurities in marketed products. However, ICH Q3A (R) is not intended for application during early clinical development, in which case several approaches can be taken to ensure toxicological cover of impurities in batches of API for clinical use. These may include the use of the same material for both animal and clinical trials or the use of a batch with lower impurity content for clinical studies than the batch used in animals. When the amount of the impurity is larger in the clinical batch then in the batch used in animals, toxicological cover can be achieved by ensuring that the actual amount of impurity administered to humans at the maximum clinical dose is less than the amount of impurity administered at the NOAEL (No Observed Adverse Effect Level) in animal studies.

In some instances additional work may be required to ensure an adequate safety profile, such as re-crystallizing the batch to reduce the impurity level below the qualification level or performing additional toxicity studies. Finally, when there is a new impurity that was not present in the material used for animal studies but the structure is known, then the qualification levels can be based on literature/database searches indicating, for example, that no known relevant human risks are associated with that structural class or substructures. Whichever approach is used to ensure that the impurity profile of the clinical batch is acceptable, it is evident that good understanding of the structural identity, levels and mechanism of formation of the main impurities is functional to the definition of the safety profile of the drug or to the implementation of process changes that could eventually produce material of an adequate quality [12–14]. To this end, the use of a wide range of different analytical techniques is a key scientific tool.

In the present work, a multi-technique analytical approach aimed at the elucidation of the structure of the major side-products present at a low-level in batches of GW876008 (1) drug substance is described. Two of these side products, present at levels close to the ICH qualification limit, were identified in the first synthetic scale-up (carried out to produce the batch for preclinical studies) by using a classic combination of LC–MS and LC–NMR. Two further new impurities were then unexpectedly discovered, at levels greater than the reporting limit of 0.05%, only in the larger clinical grade scale-up carried out to produce the batch for Phase I clinical studies. Due to their actual levels, chromatographic peak profiles and structural complexity, their identification required a multidisciplinary approach, which included not only LC–MS and LC–NMR, but also a preliminary semi-preparative separation of the two impurities, coupled with a further advanced HR–MS and HR–NMR investigation.

2. Experimental

2.1. LC–NMR

LC–NMR was performed on a Varian INOVA 600 MHz NMR spectrometer operating at 599.71 MHz for ^{1}H, coupled to a Varian Pro-Star 5 HPLC system equipped with Diode Array Detector (DAD). A PFG-IFC triple-resonance (^{1}H, ^{13}C, ^{15}N) NMR probe was used. LC–NMR was performed in stopped-flow mode. The mobile phase was constituted by (A) D_2O + 0.1% trifluoroacetic acid (TFA); (B) acetonitrile (ACN) + 0.1% TFA. A linear gradient from 0% (B) to 95% (B) in 30 min was applied at 1 ml/min flow rate. UV detection wavelength was set at 254 nm. The sample, dissolved in mobile phase at a concentration of about 1 mg/ml, was injected (100 μl) into a reversed-phase Waters X-Terra-C18 column (150 mm × 4.6 mm × 5 μm). ^{1}H NMR spectra of the two impurities of interest (Rt = 16.1 min for impurity 4; Rt = 17.7 min for impurity 5) were collected by stopping the chromatographic flow in correspondence of the UV detection peaks. ^{1}H NMR spectra were acquired using the standard WET1D sequence with double pre-saturation of both the residual water and ACN resonances. Data were acquired with 12 kHz sweep width, using 32K time-domain points with an acquisition time of 1.82 s. A number of scans of 512 (impurity 4) and 1024 (impurity 5) were used in order to achieve an adequate signal-to-noise. All spectra were collected at operating temperature of 22 °C. ^{1}H LC–NMR spectra were referenced to the ACN resonance (1.96 ppm).

2.2. HR–NMR

The sample containing the mixture of impurities (6) and (7) from semi-preparative purification was dissolved in DMSO-d_6. The addition of TFA was made directly into the NMR tube (two drops). 1D ^{1}H NMR, as well as 2D gCOSY and 2D ROESY spectra were acquired on a Varian INOVA 600 MHz NMR spectrometer operating at 599.71 MHz and utilizing a PFG 5 mm penta-probe at operating temperature of 25 °C. ^{1}H NMR spectra were acquired with a 9 kHz sweep width using 32K time-domain points with an acquisition time of 3.56 s. ^{1}H NMR spectra were referenced to the residual solvent line (2.50 ppm for DMSO-d_6). The 2D gCOSY spectrum was acquired using ^{1}H sweep width 5 kHz in $f1$ and $f2$ dimensions, with 2048 points in $f2$, 512 complex increments in $f1$, 2 scans per increment. The 2D gCOSY experiment was transformed with a sine-bell weighting function in both dimensions. The 2D ROESY spectrum was acquired using ^{1}H sweep width 5 kHz in $f1$ and $f2$ dimensions, with 2048 points in $f2$, 256 complex increments in $f1$, 8 scans per increment, mixing time of 350 ms. The 2D ROESY spectrum was transformed with a cosine squared weighting function in both dimensions, after applying zero-filling in $f1$ and $f2$ dimensions.

2.3. LC–MS and HR–MS

LC/MS measurements were carried out on an Agilent 1100 series coupled to a Q-Tof2^{TM} mass spectrometer. A Zorbax SB-Phenyl 150 mm × 4.6 mm × 3.5 μm column was used at room temperature. The mobile phase was constituted by (A), water + 0.05% TFA - (B), ACN/methanol 50/50 (v/v) + 0.05% TFA. A linear gradient from 0% (B) to 95% (B) was applied over 30 min run time at a flow rate 1 ml/min; the injection volume was 20 μl. The ionization mode was positive electrospray (ESI); collision gas was research grade Argon (Ar 5.0); collision energy was between 40 and 50 eV; internal lock mass was m/z 784.8230 $[H_{25}P_8O_{32}]^+$ generated by infusion of 0.2% solution of H_3PO_4 in ACN/water 1:1 (v/v). The resolution measured on peak m/z 807 in the HR–MS was 10070 (FWHM), while LM and HM resolution settings of the quadrupole used to carry out the MS/MS were 5.0.

2.4. HPLC-UV

GW876008 (1) batches were analysed using a reverse phase HPLC method on a Agilent 1100 HPLC system equipped with DAD detector. A Zorbax Bonus RP 150 mm × 4.6 mm × 3.5 μm column was used at 40 °C temperature. A solution of GW876008 (1) at a concentration of 0.3 mg/ml was prepared using mobile phase as the dissolving solvent. A volume of 5 μl was injected with a mass loading of 1.5 μg. The mobile phase was constituted by water + 0.05% TFA (A); ACN/methanol 50/50 (v/v) + 0.05% TFA (B). A linear gradient from 0% (B) to 95% (B) was applied over a 30 min run time, at a flow rate of 1.0 ml/min. The detection wavelength was set at 220 nm.

2.5. Semi-preparative HPLC

The separation of the two impurities (6) and (7) was performed using a reverse phase semi-preparative HPLC method on a Varian SD1 Preparative HPLC system, equipped with two 500 ml head pumps. A pre-packed Zorbax SB-Phenyl PrepHT 21.2 mm × 250 mm × 7 μm column was used. The mobile phase was constituted by water + 0.05% TFA (A); ACN/methanol 50/50% (v/v) + 0.05% TFA (B). A linear gradient from 0% (B) to 100% (B) was applied over a 30 min run time at a flow rate of 21 ml/min. The detection wavelength was set at 220 nm. A solution of GW876008 (1) at a concentration of 50 mg/ml was prepared using mobile phase as dissolving solvent. A volume of 200 μl was injected into the preparative HPLC system, with a mass loading of 10 mg. The collected fractions were dried out in a Buchi "Rotavapor".
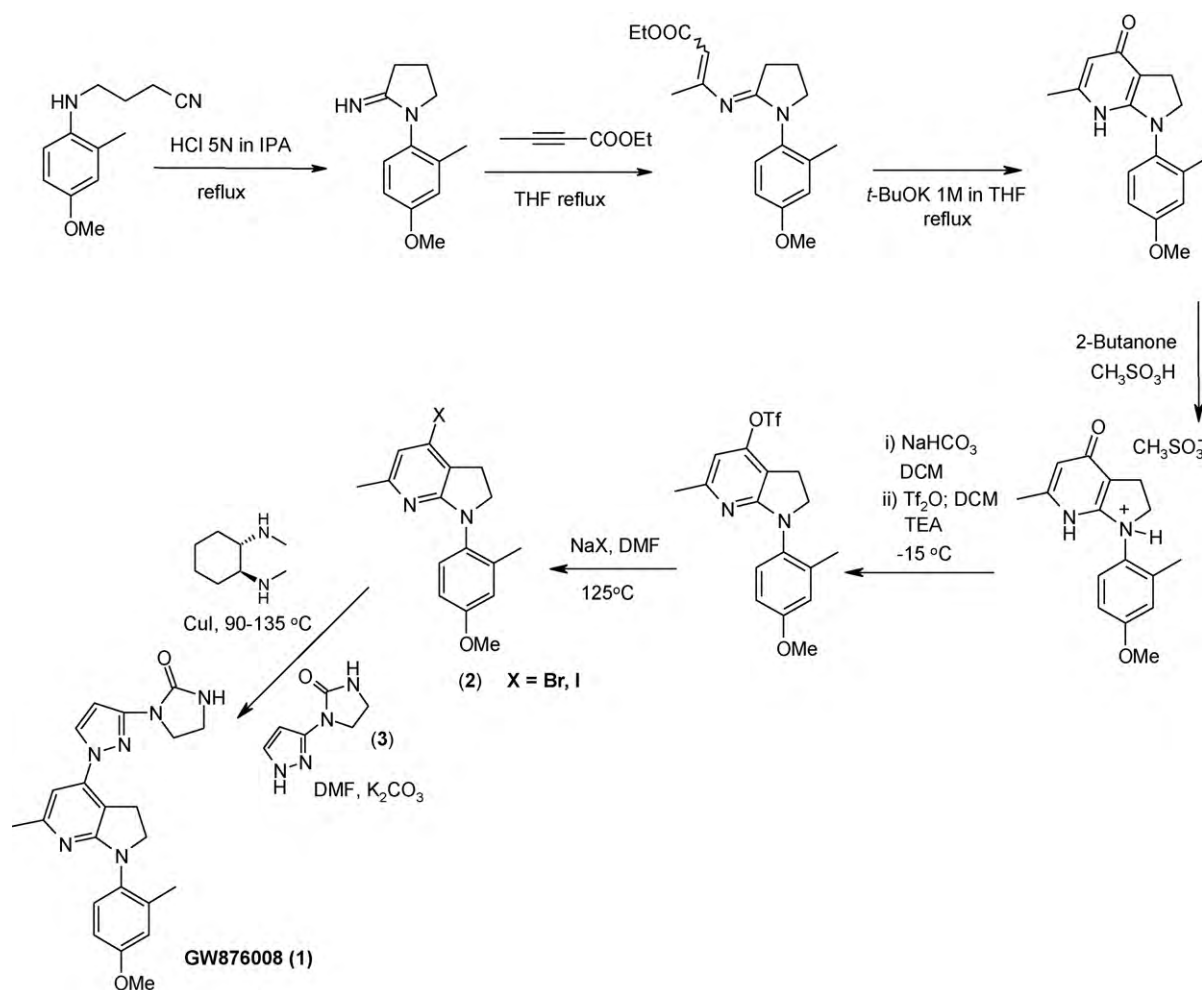
Scheme 1. Synthetic route to GW876008.

3. Results and discussion

The synthetic route used in the early large scale development for GW876008 (1) is reported in Scheme 1 [15,16].

The first multi-gram scale-up was carried out to produce the API batch for toxicological studies. Two major impurities, named impurity (4) and impurity (5) with peak relative retention times (Rrt) of 1.06 and 1.17 respectively, were found in this first batch by HPLC-UV as reported in Table 1 (batch 1).

The combined application of LC–MS and LC–NMR allowed the identification of these impurities during synthetic route assessment. LC–NMR [17–19] was applied in a stopped-flow mode, by adapting the analytical chromatographic method conditions using deuterated water (D_2O) instead of water in the mobile phase (D_2O/ACN).

The proposed structures of the two impurities, with the corresponding LC–NMR spectra, are reported in Fig. 1.

The structure of impurity (4), corresponding to a de-hydrogenated analogue of the parent compound, was determined by knowing the molecular weight from LC–MS (m/z = 403, [M+H]$^+$) and by the observation of two extra aromatic resonances and the corresponding lack of the two methylene resonances of GW876008 (1) 2,3-dihydro-1H-pyrrolo [2,3-b]pyridine bicyclic core. A chemical rationale to explain the formation of impurity (4) can be provided considering that during the synthetic process the final compound (1) is heated for several hours up to 90–135 °C in presence of a copper-catalyst and a base. These high temperature conditions are known to favour the oxidative aromatization process, since the reaction is not carried out under an oxygen-purged atmosphere [20,21].

The interpretation of the structure of impurity (5) resulted more complex in terms of simple ^{1}H NMR resonances. However, the observation of a single pyrazole couple of protons, with respect to doubled resonances for all the other aromatic protons expected for

Table 1
Impurity content in GW876008 drug substance batches determined by HPLC-UV. The batch used in toxicological studies (batch 1) and the batches intended for clinical use (batches 2 and 3) are reported. Batch 3 was obtained by preparative HPLC purification and re-crystallization of batch 2.

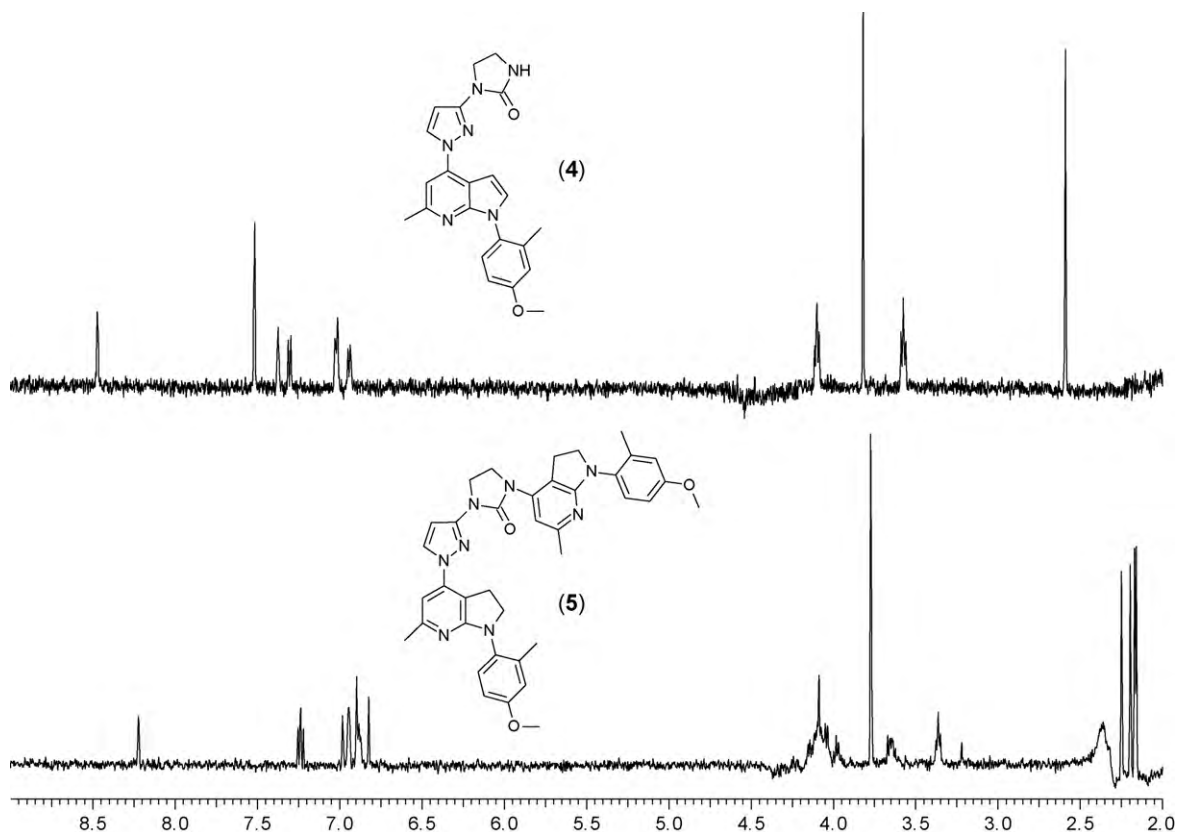| Batch	Impurity 4, Rrt 1.06 (% a/a)	Impurity 5, Rrt 1.17 (% a/a)	Impurity 6, Rrt 1.11 (% a/a)	Impurity 7, Rrt 1.12 (% a/a)
1	0.37	0.07	<0.05	<0.05
2	0.18	0.08	0.23	0.10
3	0.18	<0.05	n.d.*	n.d.*

* n.d., not detected.

Fig. 1. Stopped-flow LC–NMR results for the chromatographic peaks of impurities (4) and (5). The two spectra were collected during LC–NMR experiments by stopping the flow in correspondence of the UV detection of the impurity peaks.
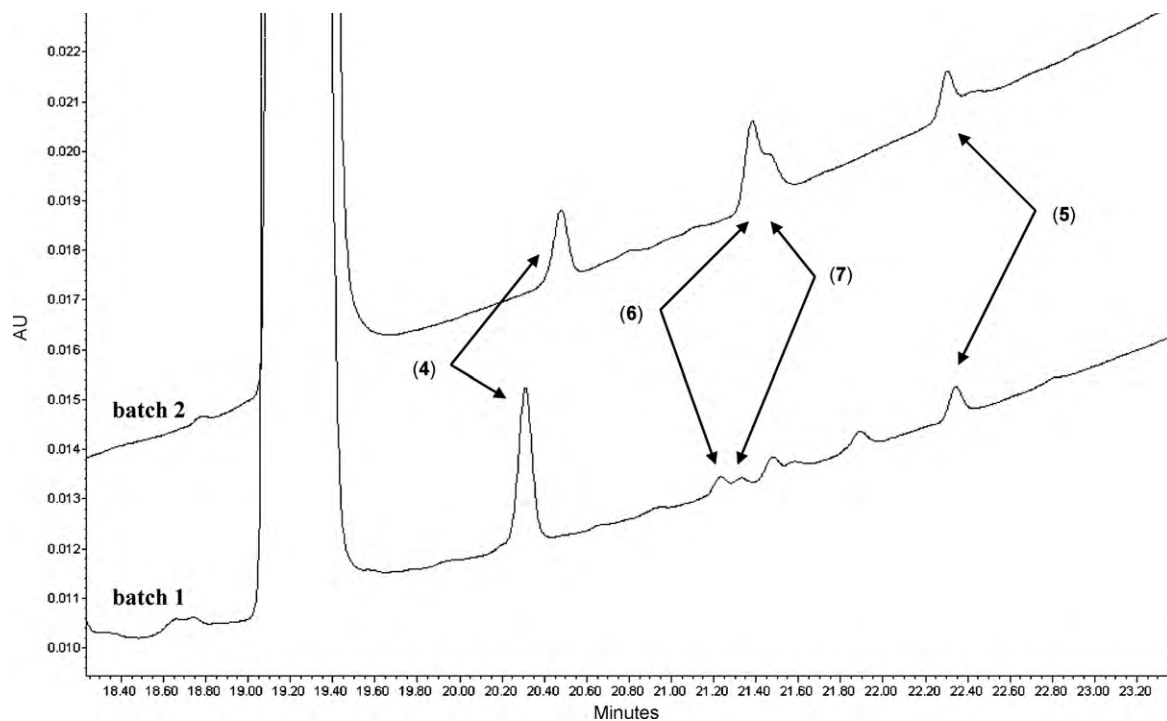

Fig. 2. Comparison of HPLC chromatograms for batches 1 and 2 respectively (see Table 1 for impurity content data) of GW876008 (1). The drug substance elutes as main peak at rt = 19.2 min. Impurities (6) and (7) were detected at trace levels in the first scale up batch (bottom trace, <0.05% a/a), while they were detected at critical levels in the larger scale batch (top trace), that is approximately at 0.23% a/a (6) and 0.10% a/a (7), respectively. Impurities (4) and (5) in both batches are also highlighted here.

the parent GW876008 (1), suggested the structure proposed here, in agreement with LC–MS data (m/z = 657, [M+H]$^+$). The integration of the methylene resonances in the region 4.2–3.2 ppm allowed us also to identify a single imidazolidin-2-one ring. The structure of this impurity was further confirmed based on a scientific rationale derived from the chemistry applied (Scheme 1), considering that the last intermediate (2) can react, under copper-catalysis with both nitrogens of pyrazolylurea (3), even if with different reaction rates [22]. Table 2 reports the ^{1}H NMR assignments as derived from LC–NMR experiments. It is worth highlighting that both these compounds were synthesized afterwards in order to both produce adequate amounts as analytical standards and to get further structure confirmation.

The larger scale synthesis of GW876008 (1), carried out to manufacture several kilograms of API for Phase I clinical studies, resulted in a batch with more complex impurity profile (see Table 1, batch 2). In fact, this batch contained the already identified impurities (4) and (5), plus two partially co-eluting new impurities (6 and 7). As shown in Fig. 2, reporting the chromatographic traces of both batches, these two new impurities had been detected also in batch 1 but at levels below 0.05% a/a (see Table 1) and therefore not considered critical at that stage of development.

Both LC–MS and LC–NMR experiments were initially performed with the aim to elucidate the chemical structures of these two new unknown impurities. However, the stopped-flow LC–NMR experiment did not allow us to gain sufficient structural insights due to the apparent increasing complexity of the resulting ^{1}H NMR spectra

and the simultaneous presence of both impurities (6) and (7) in the partially coeluting mixture. Moreover, LC–MS resulted confirmed a molecular weight of 806 for both impurities, thus suggesting that they could be two isomers of a dimeric form of GW876008 (1), with loss of two mass units (Fig. 3).

The structures of impurities (6) and (7) were therefore further investigated by means of HR-NMR following a preliminary semi-preparative HPLC purification, to reduce interference and increase sample concentration. The chromatographic fraction obtained by semi-preparative HPLC was first analyzed by dissolving the isolated material in DMSO-d_6. The ^{1}H NMR spectrum was still very complex, showing broad lines in both aromatic and aliphatic regions, plus resonances between 4.0 and 3.0 ppm, disturbed by the residual water signal. To overcome these issues, an addition of trifluoroacetic acid (TFA) to the DMSO-d_6 solution was made. This addition allowed shifting downfield the water resonance (>10 ppm) and sharpening all the signals of the two compounds (Fig. 4).

The ^{1}H NMR spectrum obtained gave some additional key information that addressed a full understanding of the two structures. Both compounds (in relative ratio of ca. 70/30 molar, in line with peak integration by HPLC-UV) presented two typical pyrazole doublets in the region 8.5–8.2 ppm. This observation confirmed that in both impurities, as dimers, the two pyrazole ring units were intact. Moreover, the [1]H–[1]H coupling constant (J = 3 Hz) measured for these pyrazole doublets indicated the same N-1 substitution as in the parent compound GW876008 (1). Analogous considerations could be made taking into account the methoxy resonances,

Table 2
^{1}H NMR assignments for impurities (4) and (5) derived from LC-NMR experiments.

Impurity (4)

Impurity (5)

^{1}H NMR (δ, ppm)[a]	Assignment	^{1}H NMR (δ, ppm)[a]	Assignment
8.47 (br.s., 1H)	24	8.22 (br.s., 1H)	24
7.52 (br.s., 2H)	2, 3	7.24 (m, 2H)	16, 16′
7.38 (m, 1H)	8	6.98 (br.s., 1H)	23
7.30 (d, 1H)	16	6.95 (m, 2H)	13, 13′
7.02 (m, 2H)	13, 23	6.90 (s, 1H)	8
6.94 (d, 1H)	15	6.88 (m, 2H)	15, 15′
4.10 (t, 2H)	29	6.82 (s, 1H)	8′
3.82 (s, 3H)	19	4.20–3.95 (m, 8H)	2, 2′, 28, 29
3.58 (t, 2H)	28	3.77 (2 s, 6H)	19, 19′
2.59 (s, 3H)	10	3.65 (m, 2H)	3′
n.d.[b]	17	3.36 (m, 2H)	3
		2.25, 2.20, 2.17, 2.16 (4 s, 12H)	10, 10′, 17, 17′

[a] Chemical shifts referenced to ACN line (1.96 ppm).
[b] Not detected, expected in the region 2.1–1.9 ppm, probably overlapped with the suppressed ACN resonance.
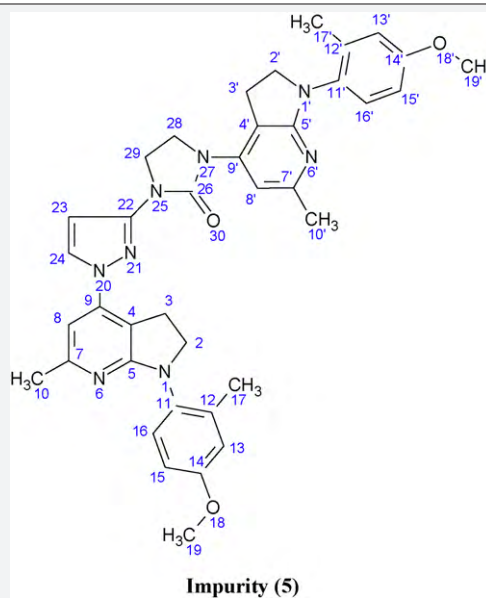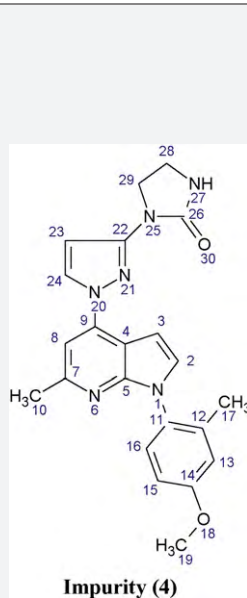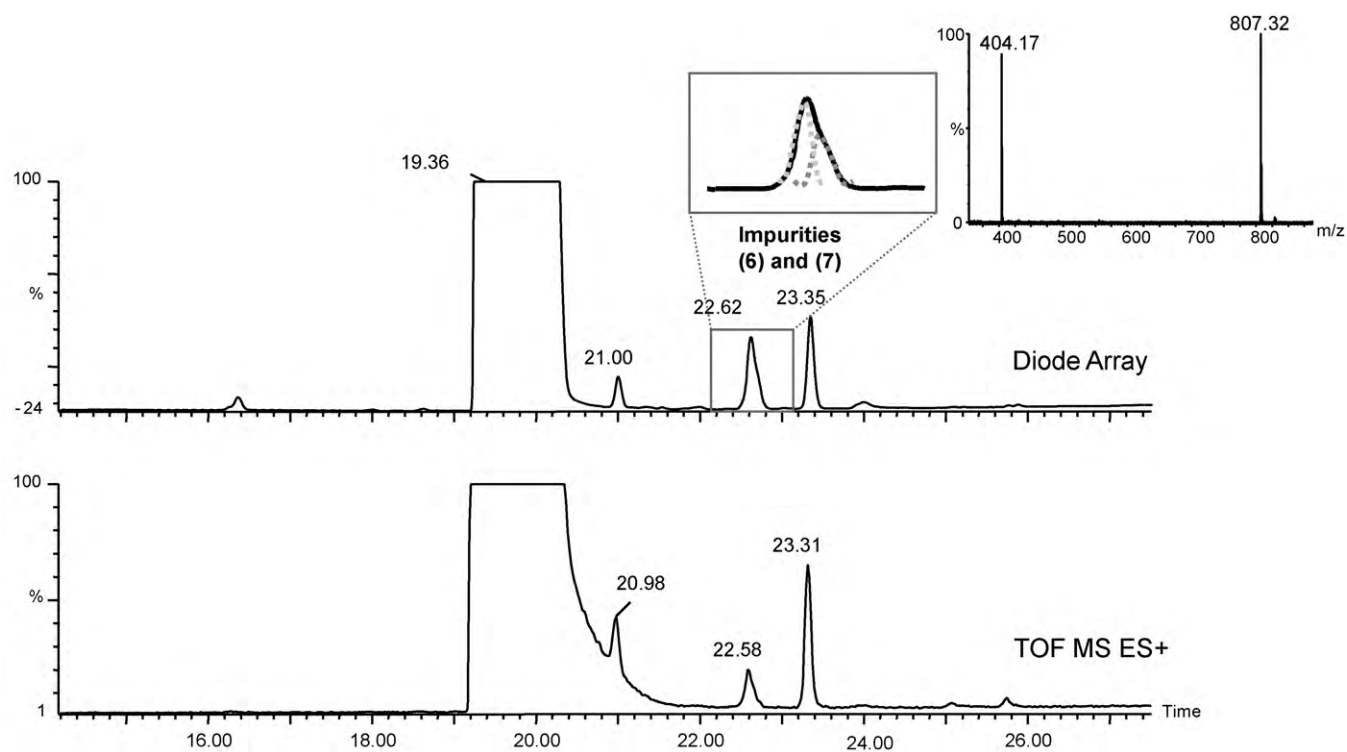
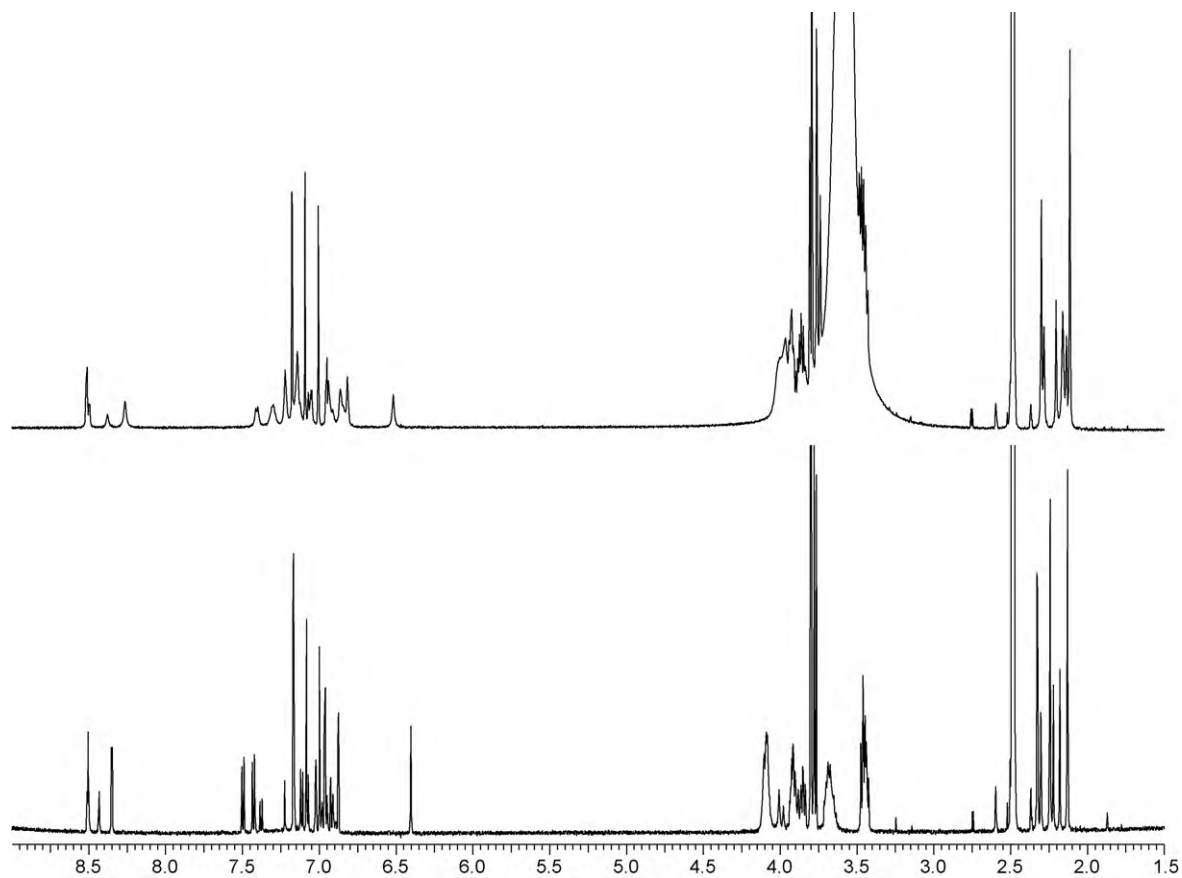**Fig. 3.** LC–MS results for the impurities (6) and (7).

Fig. 4. ^{1}H NMR spectra in DMSO-d_6 (top) and in DMSO-d_6 + TFA (bottom) of the purified fraction containing the mixture of impurities (6) and (7).
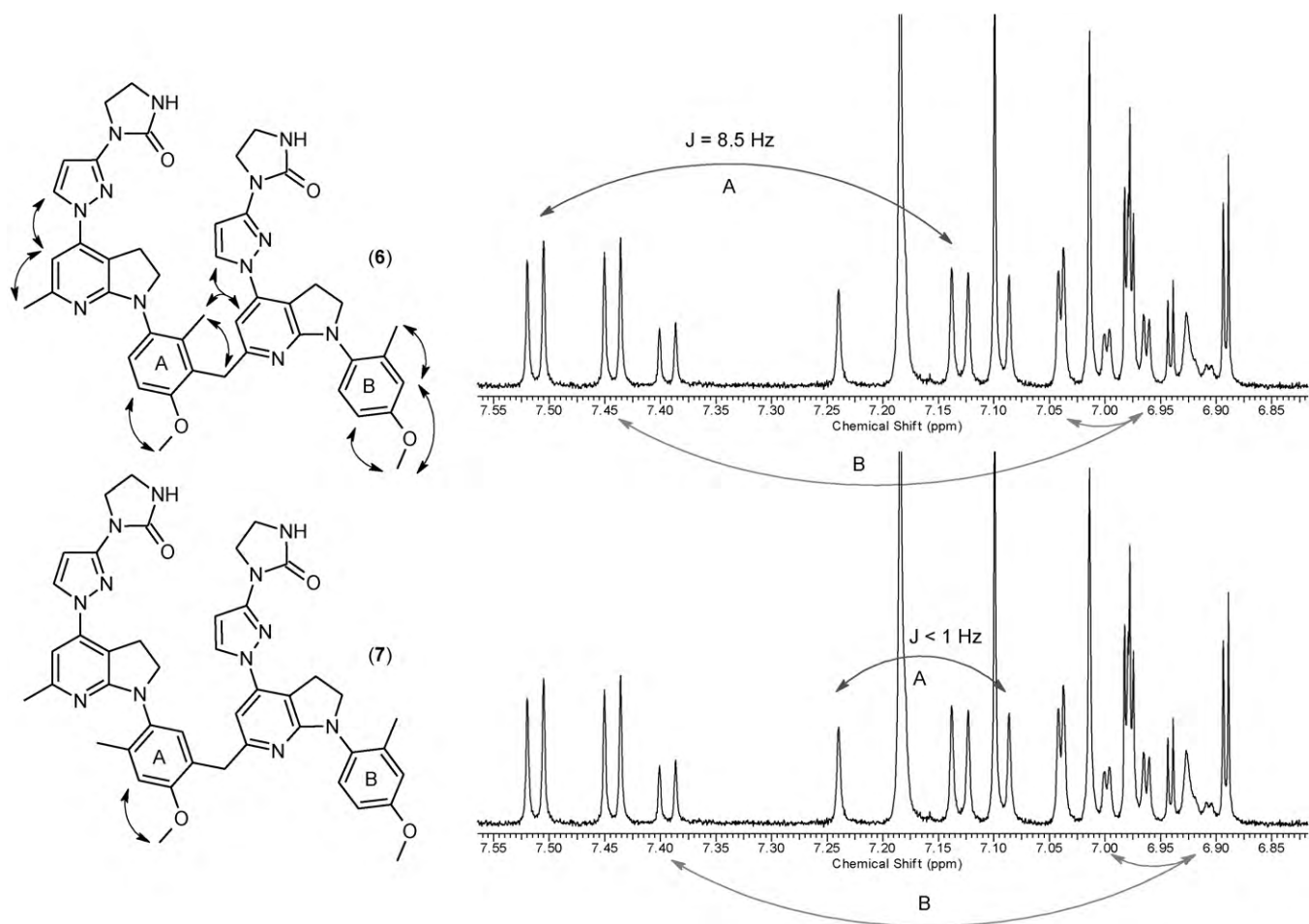
Fig. 5. ¹H NMR expanded plot of the aromatic region. The spectra on the right report the highlighted aryl (A) and (B) resonances for impurities (6) and (7) on top and bottom, respectively. The most relevant nOe's from the 2D ROESY experiment are also highlighted on the two structures reported on the left. An approximate 70/30 ratio [(6)/(7)] can be measured from ¹H integration.
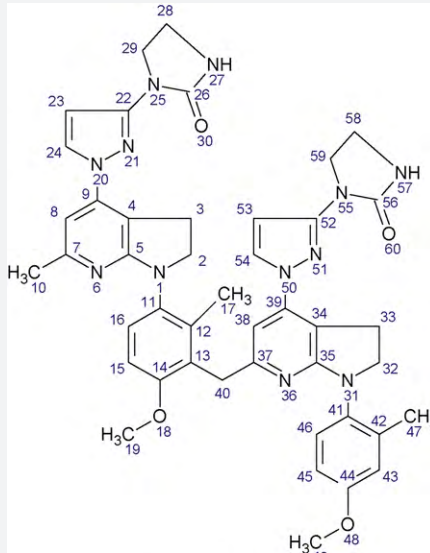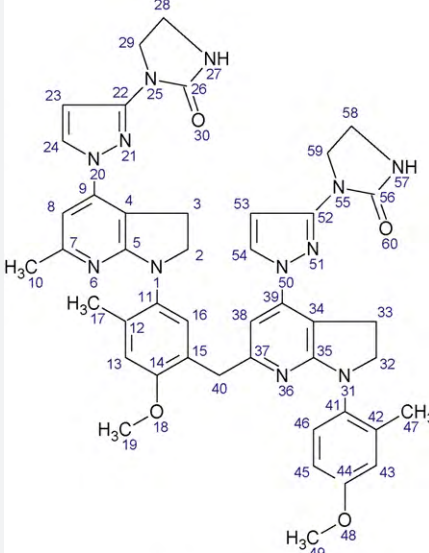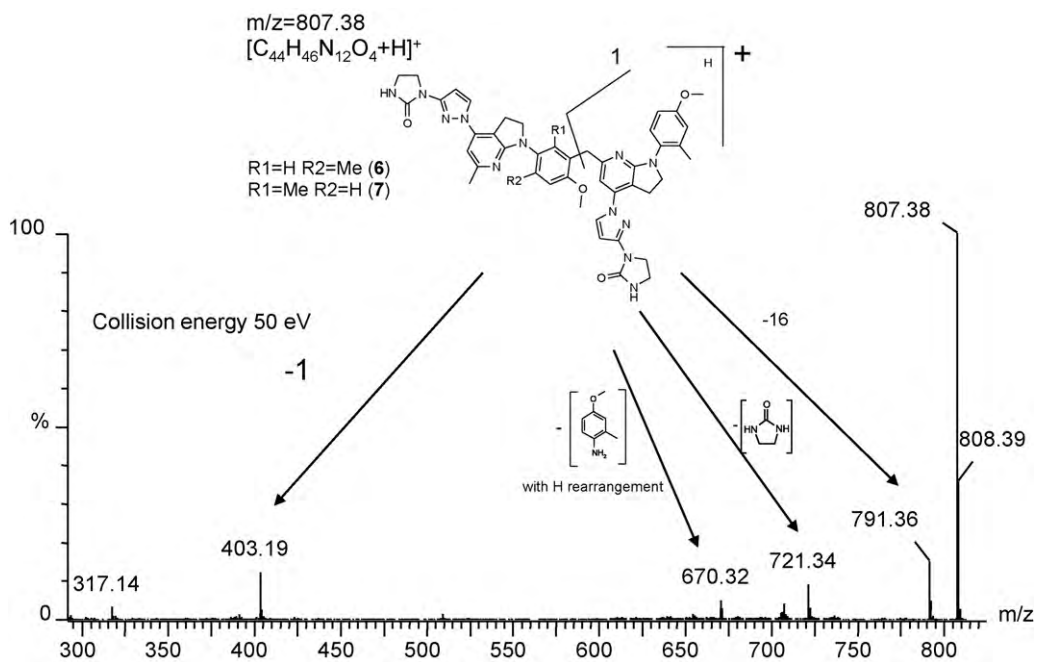

Fig. 6. MS/MS spectrum and relevant fragments assignment for impurities (6) and (7).

Table 3
^{1}H NMR assignments for impurities (**6**) and (**7**) derived from HR-NMR experiments on the purified fraction.

Impurity (6)

Impurity (7)

^{1}H NMR (δ, ppm)[a]	Assignment	^{1}H NMR (δ, ppm)[a]	Assignment
8.52 (d, 1H)	24	8.52 (d, 1H)	24
8.36 (d, 1H)	54	8.45 (d, 1H)	54
7.51 (d, 1H)	16	7.39 (d, 1H)	46
7.44 (d, 1H)	46	7.24 (s, 1H)	16
7.18 (s, 1H)	8	7.18 (s, 1H)	8
7.13 (d, 1H)	15	7.09 (s, 1H)	13
7.04 (d, 1H)	43	7.00 (d, 1H)	43
6.98 (d, 1H)	23	6.96 (d, 1H)	23
6.97 (dd, 1H)	45	6.94 (d, 1H)	53
6.89 (d, 1H)	53	6.93 (br.s., 1H)	38
6.42 (s, 1H)	38	6.91 (m, 1H)	45
4.11 (m, 5H)	29, 59, 40′	4.11 (m, 4H)	29, 59
4.01 (d, 1H)	40″	3.91 (m, 6H)	2, 32, 40
3.90 (m, 4H)	2, 32		
3.81 (s, 3H)	49	3.82 (s, 3H)	19
3.80 (s, 3H)	19	3.78 (s, 3H)	49
3.69 (m, 4H)	28, 58	3.69 (m, 4H)	28, 58
3.47 (m, 4H)	3, 33	3.47 (m, 4H)	3, 33
2.34 (s, 3H)	10	2.32 (s, 3H)	10
2.26 (s, 3H)	47	2.24 (s, 3H)	17
2.15 (s, 3H)	17	2.20 (s, 3H)	47

[a] Spectra collected in DMSO-d_6 + TFA, chemical shifts referenced to residual DMSO line (2.50 ppm).

which are two for each impurity. Moreover, for each of the two impurities in the mixture: (a) one proton was missing considering the integration of the aromatic region; (b) an extra methylene was present considering the integration in the region 4.2–3.2 ppm; (c) three aryl-methyl singlets could be counted easily. Finally, 2D gCOSY and 2D ROESY experiments allowed full assignment of ^{1}H NMR resonances for these impurities (Table 3) suggesting the two molecular structures reported in Fig. 5.

In particular, the aryl substitution involving the former 2,3-dihydro-1H-pyrrolo[2,3-b]pyridine methyl in position *ortho* (6) and *para* (7) with respect to the aryl methyl was demonstrated by evaluation of the coupling constants of the aromatic protons as well as by the analysis of the dipolar correlations in the 2D ROESY experiment (Fig. 5).

In addition, MS/MS fragmentation pathway (Fig. 6) and HR-MS were performed on the material after semi-preparative purification. The HR-MS determination gave a mass value of 807.3839, in agreement with a molecular formula of $C_{44}H_{47}N_{12}O_4$ (double bond equivalent, DBE = 28 for the neutral molecular formula $C_{44}H_{46}N_{12}O_4$), with a mass shift of -0.6 ppm with respect to the

calculated mass of 807.3843. These HR–MS experiments further confirmed the two proposed structures (6) and (7).

Based on the proposed structures, the formation of the two impurities (6) and (7) can be explained as the result of a non-regioselective cross-dehydrogenative coupling between a sp[3] C–H bond and a sp[2] C–H bond, through the C–H activation of the sp[3] bond. This chemical process appear to be challenging due to the low reactivity of C(sp[3])-H bond and the lack of coordination for the transition-metal catalyst. However, based on the synthetic chemistry conditions, we can hypothesize that the copper-diamine complex acts as a base for the deprotonation of the C–H bond to prompt phenylation of the 2-methyl group [23].

4. Conclusions

A multi-technique approach was applied in order to fully characterize four low-level unknown impurities of GW876008, a novel CRF$_1$ receptor antagonist. LC-MS and LC-NMR proved their efficiency as fast methods to determine the structures of two major impurities in GW876008 (1) drug substance batches. Information

obtained by coupling the LC–MS experiment with the simple ^{1}H NMR spectrum in stopped-flow LC–NMR, was sufficient for the elucidation of the two main side-products in the first scale-up process, for preclinical use. More experimental work was needed instead to investigate the structures of the other two new impurities found in a second larger scale synthesis, for clinical use. These impurities were identified as two regioisomers of a dimer of GW876008 (1). HR–MS and HR–NMR were used to produce this result by directly analyzing, after semi-preparative purification, the mixture of the almost co-eluting regioisomers without the need for a further development of the method used for their separation. The outcome of these studies allowed us to set up opportune batch purification and improve the synthetic process. In particular, batch 2 was purified by large scale preparative HPLC and recrystallized to eliminate the impurity excess and obtain a material with a safety profile suitable for clinical trials (see Table 1, batch 3). The use of a wide range of different analytical and spectroscopy techniques, including LC–NMR, LC–MS, semi-preparative HPLC, HR–NMR and HR–MS, proved to be a key scientific tool in terms of complex impurity structural investigations, resulting in more effective support for the early development package of new synthetic chemical entities.

Acknowledgements

References

[1] M.J. Owen, C.B. Nemeroff, Physiology and pharmacology of corticotropin-releasing factor, Pharmacol. Rev. 43 (1991) 425–473.

[2] E.B. De Souza, Corticotropin-releasing factor receptors: physiology, pharmacology, biochemistry and role in central nervous system and immune disorders, Psychoneuroendocrinology 20 (1995) 789–819.

[3] F. Holsboer, The rationale for corticotropin-releasing hormone receptor (CRH-R) antagonists to treat depression and anxiety, J. Psychiatr. Res. 33 (1999) 181–214.

[4] R. Di Fabio, Y. St-Denis, F.M. Sabbatini, D. Andreotti, R. Arban, G. Bernasconi, S. Braggio, F.E. Blaney, A.M. Capelli, E. Castiglioni, E. Di Modugno, D. Donati, E. Fazzolari, E. Ratti, A. Feriani, S. Contini, G. Gentile, D. Ghirlanda, S. Provera, C. Marchioro, K.L. Roberts, A. Mingardi, M. Mattioli, A. Nalin, F. Pavone, S. Spada, D.G. Trist, A. Worby, Synthesis and pharmacological characterization of novel druglike corticotropin-releasing factor 1 antagonists, J. Med. Chem. 51 (2008) 7370–7379.

[5] F. Qiu, D.L. Norwood, Identification of pharmaceutical impurities, J. Liq. Chromatogr. Relat. Technol. 30 (2007) 877–935.

[6] S. Görög, Chemical and analytical characterization of related organic impurities in drugs, Anal. Bioanal. Chem. 377 (2003) 852–862.

[7] K.M. Alsante, T.D. Hatajik, L.L. Lohr, T.R. Sharp, Isolation and identification of process related impurities and degradation products from pharmaceutical drug candidates, Part I, Am. Pharmaceut. Rev. 4 (2001) 70–78.

[8] L.L. Lohr, T.R. Sharp, K.M. Alsante, T.D. Hatajik, Isolation and identification of process related impurities and degradation products from pharmaceutical drug candidates: Part II. The roles of NMR and Mass Spectrometry, Am. Pharmaceut. Rev. Fall issue (2001) 104–113.

[9] D. Bartos, S. Görög, Recent advances in the impurity profiling of drugs, Curr. Pharm. Anal. 4 (2008) 215–230.

[10] S. Vasanti, S. Sulabha, Impurity profile—a review, Drug Invention Today 1 (2009) 81–88.

[11] Q3A (R2): Impurities in New Drug Substances, ICH Harmonized Tripartite Guideline, 2006.

[12] N. Mistry, I.M. Ismail, M.S. Smith, J.K. Nicholson, J.C. Lindon, Characterisation of impurities in bulk drug batches of fluticasone propionate using directly coupled HPLC-NMR spectroscopy and HPLC-MS, J. Pharm. Biomed. Anal. 16 (1997) 697–705.

[13] P. Novak, P. Tepeš, I. Fistrić, I. Bratoš, V. Gabelica, The application of LC–NMR and LC–MS for the separation and rapid structure elucidation of an unknown impurity in 5-aminosalicylic acid, J. Pharm. Biomed. Anal. 40 (2006) 1268–1272.

[14] P. Novak, P. Tepeš, M. Ilijaš, I. Fistrić, I. Bratoš, A. Avdagić, Z. Hameršak, V. Gabelica Marković, M. Dumić, LC–NMR and LC–MS identification of an impurity in a novel antifungal drug icofungipen, J. Pharm. Biomed. Anal. 50 (2009) 68–72.

[15] D. Andreotti, S. Bacchi, M. Delpogetto, S. Guelfi, A. Perboni, A. Ribecai, S. Spada, P. Stabile, M. Tampieri, Process for preparing heterocyclylpyrrolopyridines and their use as antagonists of corticotropin-releasing factor (CRF) receptors. PCT Int. Appl. WO 2006108689, 42 p. (2006).

[16] S. Bacchi, M. Delpogetto, S. Guelfi, A. Perboni, A. Ribecai, P. Stabile, M. Tampieri, Process for preparation of heterocyclylpyrrolopyridines from halopyrrolopyridines using copper catalysts, PCT Int. Appl. WO 2006108693, 37 p. (2006).

[17] J.C. Lindon, J.K. Nicholson, I.D. Wilson, Direct coupling of chromatographic separations to NMR spectroscopy, Prog. Nucl. Magn. Reson. Spectrosc. 29 (1996) 1–49.

[18] K. Albert, On-line use of NMR detection in separation chemistry, J. Chromatogr. A 703 (1995) 123–147.

[19] K. Albert, On-Line LC-NMR and Related Techniques, John Wiley & Sons, Chichester, 2002.

[20] Y. Maeda, T. Nishimura, S. Uemura, Copper-catalyzed oxidation of amines with molecular oxygen, Bull. Chem. Soc. Jpn. 76 (2003) 2399–2403.

[21] Y. Nomura, Y. Kawashita, M. Hayashi, Efficient synthesis of substituted indoles and benzazoles by oxidative aromatization using activated carbon-molecular oxygen system, Heterocycles 74 (2007) 629–635.

[22] C.C. Lee, P.S. Wang, M.B. Viswanath, M. Leung, Synthesis of symmetrical and unsymmetrical N-aryl-substituted cyclic ureas through copper(I) iodide catalyzed Goldberg-Buchwald-Nandakumar C-N coupling reactions, Synthesis 9 (2008) 1359–1366.

[23] Z. Li, C.J. Li, CuBr-catalysed direct indolation of tetrahydroisoquinolines via cross-dehydrogenative coupling between sp^3 C–H and sp^2 C–H bonds, J. Am. Chem. Soc. 127 (2005) 6968–6969.